Cell. Mol. Life Sci. (2010) 67:907–918
DOI 10.1007/s00018-009-0220-2

Cellular and Molecular Life Sciences

RESEARCH ARTICLE

Connexin32 hemichannels contribute to the apoptotic-to-necrotic transition during Fas-mediated hepatocyte cell death

Mathieu Vinken · Elke Decrock · Elke De Vuyst · Marijke De Bock · Roosmarijn E. Vandenbroucke · Bruno G. De Geest · Joseph Demeester · Niek N. Sanders · Tamara Vanhaecke · Luc Leybaert · Vera Rogiers

Received: 20 May 2009 / Revised: 16 November 2009 / Accepted: 18 November 2009 / Published online: 4 December 2009

Abstract The present study was set up to investigate the fate of connexin32 and its channels in hepatocellular apoptosis. Primary hepatocyte cultures were exposed to Fas ligand and cycloheximide, and modifications in connexin32 expression and localization, and gap junction functionality were studied. We found that gap junction functionality rapidly declined upon progression of cell death, which was associated with a decay of the gap junctional connexin32 protein pool. Simultaneously, levels of newly synthesized connexin32 protein increased and gathered in a hemichannel configuration. This became particularly evident towards the end stages of the cell death process and was not reflected at the transcriptional level. We next either silenced connexin32 expression or inhibited connexin32 hemichannel activity prior to cell death induction. Both approaches resulted in a delayed termination of the cell death response. We conclude that connexin32 hemichannels facilitate the apoptotic-to-necrotic transition, which typically occurs in the final stage of hepatocellular apoptosis.

Keywords Apoptosis · Primary hepatocyte · Connexin32 · Gap junction · Hemichannel

M. Vinken (✉) · T. Vanhaecke · V. Rogiers
Department of Toxicology, Faculty of Medicine and Pharmacy, Vrije Universiteit Brussel, Laarbeeklaan 103, 1090 Brussels, Belgium
e-mail: mvinken@vub.ac.be

E. Decrock · E. De Vuyst · M. De Bock · L. Leybaert
Physiology Group, Department of Basic Medical Sciences, Faculty of Medicine and Health Sciences, Ghent University, De Pintelaan 185, 9000 Ghent, Belgium

R. E. Vandenbroucke
Department for Molecular Biomedical Research, Ghent University-VIB, Technologiepark 927, 9052 Ghent, Belgium

B. G. De Geest · J. Demeester · N. N. Sanders
Laboratory of General Biochemistry and Physical Pharmacy, Faculty of Pharmaceutical Sciences, Ghent University, Harelbekestraat 72, 9000 Ghent, Belgium

B. G. De Geest
Laboratory of Pharmaceutical Technology, Faculty of Pharmaceutical Sciences, Ghent University, Harelbekestraat 72, 9000 Ghent, Belgium

N. N. Sanders
Laboratory of Gene Therapy, Faculty of Veterinary Medicine, Ghent University, Heidestraat 19, 9820 Merelbeke, Belgium

Abbreviations

Ac-DEVD-AFC	Acetyl-Asp-Glu-Val-Asp-7-amino-4-trifluoromethylcoumarin
ATP	Adenosine triphosphate
CHX	Cycloheximide
Cx	Connexin
FasL	Fas ligand
FRAP	Fluorescence recovery after photobleaching
GAPDH	Glyceraldehyde-3-phosphate dehydrogenase
GJIC	Gap junctional intercellular communication
HBSS–Hepes	Hank's balanced salt solution supplemented with Hepes
LDH	Lactate dehydrogenase
PbAE1	1,4-Butanediol diacrylate-based poly-beta-aminoester
PBS	Phosphate-buffered saline solution

$PBSD^{+}$	Divalent ion-supplemented PBS
qRT-PCR	Quantitative real-time reverse transcriptase-polymerase chain reaction
siRNA	Small interfering RNA
TBS	Tris-buffered saline solution

Introduction

Liver homeostasis basically relies on the critical balance between cell growth, cellular differentiation and cell death. The latter mainly occurs through apoptosis, a well-orchestrated process that depends on the molecular actions of caspase proteins [1]. One of the most prominent signaling pathways that drives apoptosis in liver is initiated by binding of a specific subset of ligands, such as the Fas ligand (FasL), to their corresponding receptors at the cell membrane surface. Hepatocytes strongly express the Fas receptor, and its ligand binding results in the induction of caspase 8. Activated caspase 8 then triggers caspase 3, which subsequently cleaves a broad spectrum of cellular proteins, giving rise to the apoptotic phenotype [2, 3]. In normal liver, the prevalence of apoptosis is very low, affecting 0.05–0.1% of all liver cells in rodents [4]. During a variety of liver pathologies as well as upon exposure to hepatotoxicants, however, apoptotic activity drastically increases, which is frequently associated with elevated FasL levels [2, 3].

Gap junctions are indispensable gatekeepers of liver homeostasis. These communicating cell junctions mediate the direct intercellular exchange of small and hydrophilic molecules (e.g., second messengers), a flux called gap junctional intercellular communication (GJIC). Gap junctions are composed of two hemichannels, so-called connexons, of neighboring cells, which in turn are built up by six connexin (Cx) subunits. More than 20 mammalian connexins have so far been characterized and they are named according to their molecular weight. Connexin species known to be expressed in human and rodent liver include Cx32, Cx26, Cx43, Cx40, Cx37, Cx39, and Cx31.9/Cx30.2. Among these, Cx32 constitutes about 90% of the total hepatic connexin amount and is abundantly expressed by hepatocytes. Cx32-based gap junctions have been repeatedly found to act as key players in charge of hepatocyte proliferation and functioning [5, 6]. Their contribution in the occurrence of hepatocyte cell death, however, has so far been poorly documented [6, 7].

Overall, conflicting results have been published with respect to the role of gap junctions in apoptosis, as some groups observed a positive correlation between GJIC and apoptotic activity, whereas others showed that gap junctions rather counteract this process [5, 8, 9]. To make the picture even more complicated, accumulating evidence points to the participation of hemichannels in apoptotic cell death. Hemichannels have long been considered as merely structural precursors for gap junctions, but a large body of compelling evidence now clearly demonstrates that connexons themselves also provide a pathway for communication, albeit between the intracellular compartment and the extracellular environment [5, 9–11]. Although a limited number of reports have described cytoprotective functions for hemichannels [11, 12], the vast majority of currently available data indicate that connexons are actively involved in the spread of apoptosis [9–11, 13–17].

The present study was set up to investigate the role of Cx32 and its channels in Fas-mediated hepatocyte cell death. We addressed primary hepatocyte cultures as an experimental setting, as this system allows the monitoring of the entire time course of apoptosis. Indeed, apoptotic hepatocytes are barely detectable in vivo, as they are too rapidly engulfed by neighboring phagocytes [18–20]. We provide an in-depth scenario of the FasL-induced changes in hepatocellular Cx32 expression, localization, and function. We demonstrate for the first time the presence of Cx32 hemichannels in hepatocytes, and we concomitantly show that they are actively involved in the late phases of Fas-mediated cell death.

Materials and methods

Chemicals and reagents

FasL (produced in HEK293 cells and similar to natural human FasL) and cycloheximide (CHX) came from Alexis (Switzerland) and Sigma (Belgium), respectively. Acetyl-Asp-Glu-Val-Asp-7-amino-4-trifluoromethylcoumarin (Ac-DEVD-AFC) was purchased from Merck (Belgium). Propidium iodide, Hoechst 33342 and calcein–acetoxymethyl ester were from Invitrogen (Belgium), whereas Annexin V Fluos and Annexin V Alexa 568 were obtained from Roche (Germany). The ^{32}Gap27 peptide (SRPTEKTVFT) was synthesized by Thermo Fisher Scientific (Germany). The 1,4-butanediol diacrylate-based poly-beta-aminoester (PbAE1) was synthesized as described elsewhere [21]. All other chemicals were commercially available products of analytical grade and were supplied by Sigma, unless specified otherwise.

Hepatocyte cultivation and cell death induction

Procedures for the housing of rats, and isolation and cultivation of hepatocytes were approved by the local ethical committee of the Vrije Universiteit Brussel (Belgium). Male outbred Sprague–Dawley rats (Charles River

Laboratories, Belgium) were kept under controlled environmental conditions with free access to food and water. Hepatocytes were isolated by use of a two-step collagenase method, and cell viability was assessed by trypan blue exclusion [22]. Viable (≥85%) hepatocytes were plated at a density of 0.56×10^5 cells/cm^2 in William's medium E (Invitrogen, Belgium) supplemented with 7 ng/ml glucagon, 292 mg/ml L-glutamine, antibiotics (7.33 I.E./ml sodium benzyl penicillin, 50 μg/ml kanamycin monosulfate, 10 μg/ml sodium ampicillin, 50 μg/ml streptomycin sulfate) and 10% v/v fetal bovine serum. After 4 and 24 h, the cell culture medium was removed and replaced by serum-free medium supplemented with 25 μg/ml hydrocortisone sodium hemisuccinate and 0.5 μg/ml insulin (hepatocyte culture medium). Cell death was induced 44 h post-plating by renewal with hepatocyte culture medium containing 200 ng/ml FasL and 2 μg/ml CHX. Sampling was performed at the start of cell death induction, and at 2, 4, and 6 h thereafter.

Gene silencing by small interfering RNA (siRNA)

Cx32 expression was suppressed by siRNA treatment with On-target plus smart pool siRNA (accession number NM_017251) from Dharmacon (Belgium) containing a mixture of four siRNA duplexes directed against rat *gjb1*. Preparation of PbAE1/siRNA complexes (N:P ratio 50:1) was carried out as previously described [21]. The siRNA transfection was started 4 h after cell seeding by replacing the initial culture medium by hepatocyte culture medium containing the PbAE1/siRNA complexes (final siRNA concentration 100 nM). After 4 h, the culture medium was removed and replaced by regular hepatocyte culture medium. The hepatocyte culture medium was renewed once more (16 h post-transfection) prior to cell death induction (44 h post-plating). Experiments using non-targeting siRNA (Dharmacon, Belgium) were performed in parallel.

Determination of the apoptotic and necrotic indices

Hepatocyte cultures were washed twice with phosphate-buffered saline solution (PBS) containing 1.2 mM $CaCl_2$ and 340 μM $MgCl_2.6H_2O$ ($PBSD^+$). Subsequently, cells were stained with 2% v/v Annexin V Fluos, 3 μg/ml Hoechst 33342 and 1 μg/ml Propidium iodide in Annexin V buffer (140 mM NaCl, 5 mM $CaCl_2$, 10 mM Hepes) for 15 min at room temperature. Culture dishes were thereafter rinsed with $PBSD^+$ and subjected to fluorescence microscopy (Nikon, Japan). At least five images per culture dish were taken. The number of cells, positive for the concerned marker, was counted in each image and expressed relative to the total number of nuclei present.

Measurement of caspase 3-like activity

Caspase 3-like activity in primary hepatocyte cultures was measured fluorometrically by using the Ac-DEVD-AFC substrate as described elsewhere [23]. The enzyme activity was expressed as nmol AFC/min × μg protein.

Measurement of lactate dehydrogenase (LDH) leakage

Hepatocyte membrane damage was evaluated by determination of the LDH index [24], using a commercially available kit (Merck, Germany). The LDH index was calculated by the following equation: (100 × LDH activity in supernatant)/[LDH activity in (supernatant + cells)].

Fluorescence recovery after photobleaching (FRAP)

For FRAP analysis, cultured hepatocytes were loaded with 10 μM calcein–acetoxymethyl ester in Hank's balanced salt solution buffered with Hepes (HBSS–Hepes; 0.81 mM $MgSO_4.7H_2O$, 0.95 mM $CaCl_2.2H_2O$, 137 mM NaCl, 0.18 mM $Na_2HPO_4.2H_2O$, 5.36 mM KCl, 0.44 mM KH_2PO_4, 5.55 mM D-glucose, 25 mM Hepes) for 30 min at room temperature. In order to detect and thus to specifically study apoptotic cells, hepatocytes were stained with 2% v/v Annexin V Alexa 568 in Annexin V buffer for 15 min at room temperature. After extensive rinsing, cultures were kept for 10 min in HBSS–Hepes. Fluorescence within a single cell was photobleached by 1 s spot exposure to 488 nm Argon laser light, and dye influx from neighboring cells was recorded over the next 5 min with a ×40 water immersion objective (Nikon, Japan). Fluorescence in the bleached cell was expressed as the percentage recovery relative to the prebleach level. At least six cells per culture dish were examined.

Measurement of extracellular adenosine triphosphate (ATP)

ATP was measured using a commercial luciferin/luciferase assay kit (Sigma). Briefly, cultured hepatocytes were washed with divalent-free buffer (137 mM NaCl, 0.18 mM $Na_2HPO_4.2H_2O$, 5.36 mM KCl, 0.44 mM KH_2PO_4, 4 mM ethylene glycol tetra-acetic acid, 5.55 mM D-glucose, 25 mM Hepes) and incubated for 2.5 min with divalent-free buffer at room temperature. For baseline measurements, divalent-free buffer was replaced by HBSS–Hepes. After 2.5 min, ATP assay mix in HBSS–Hepes was added and luminescence was measured. ATP release was expressed as the percentage of ATP release triggered by divalent-free medium.

Cell surface biotinylation assay

Cell surface connexins in cultured hepatocytes were biotinylated and isolated using a commercially available kit, according to the manufacturer's instructions (Pierce, USA). Protein concentrations were determined according to the Bradford procedure [25], using a Bio-Rad protein assay kit (Bio-Rad, Germany) and Cx32 immunoblot analyses were performed as described hereafter.

Western blotting

For preparation of total protein lysates, cultured hepatocytes were washed with ice-cold PBS, scraped with Laemmli buffer (125 mM Tris, 80 mM sodium dodecyl sulfate, 10% v/v glycerol) and sonicated on ice for 30 s. For separation of Triton X-100 soluble and Triton X-100 insoluble fractions, cultured hepatocytes were washed with ice-cold PBS, and were harvested in cold 1% v/v Triton X-100 in PBS supplemented with 50 mM sodium fluoride, 1 mM sodium orthovanadate, 1% v/v protease inhibitor cocktail (Sigma), 1% v/v phosphatase inhibitor cocktail (Sigma), and ethylenediamine tetra-acetic acid-free protease inhibitor cocktail (Roche, Germany). Separation into Triton X-100 soluble and Triton X-100 insoluble fractions was performed by centrifugation at 16,060*g* at 4°C for 10 min. Triton X-100 insoluble fractions were resuspended in Laemmli sample buffer and sonicated on ice for 30 s. Protein concentrations were determined according to the Bradford procedure [25], using a Bio-Rad protein assay kit (Bio-Rad). Proteins were fractionated on sodium dodecyl sulfate polyacrylamide and blotted afterwards onto nitrocellulose membranes (Amersham, UK). Blocking of the membranes was performed with 5% w/v non-fatty milk in Tris-buffered saline solution (TBS; 20 mM Tris, 135 mM NaCl) containing 0.1% v/v Tween 20. Membranes were incubated overnight at 4°C with a polyclonal anti-rat Cx32 antibody (Sigma) followed by incubation for 1 h at room temperature with a horseradish peroxidase-conjugated goat anti-rabbit IgG (Dako, Denmark). Excessive antibody was removed by washing the membranes in Tween-supplemented TBS. Detection of the proteins was carried out by means of an enhanced chemiluminescence western blotting system (Amersham). For semi-quantification of the results of the Cx32 localization experiments (Triton X-100 insoluble fraction and biotinylated cell surface fraction), Cx32 blots were scanned and analyzed using the Quantity One software (Bio-Rad), and signals at indicated time points were expressed as fold change of the Cx32 signal at the start of cell death induction. For semi-quantification of the results of the Cx32 expression experiments, Cx32 blots were further incubated with a monoclonal anti-mouse glyceraldehyde-3-phosphate dehydrogenase (GAPDH) antibody (Abcam, UK), whereby Cx32 signals of treated (cell death) cultures were normalized to the corresponding GAPDH signals and were expressed as fold change of the normalized Cx32 signals in untreated (control) cultures.

Immunocytochemistry

Hepatocytes, grown on glass coverslips, were fixed for 10 min with ice-cold ethanol (70% v/v). Following rehydration with PBS, cells were permeabilized with 0.1% v/v Triton X-100 and blocked with 0.1% w/v non-fatty milk, each for 30 min. Cells were then incubated with a polyclonal anti-rat Cx32 antibody (Sigma) for 2 h, washed with PBS, and exposed to a fluorescein isothiocyanate-conjugated donkey anti-rabbit antibody (Jackson Immunoresearch Laboratories, USA) for 45 min. After extensive rinsing with PBS, samples were mounted with Vectashield containing diamidinophenylindole (Vector Laboratories, USA). Detection was performed by fluorescence microscopy (Leica DMR/XA, Germany) at ×630 magnification. For negative controls, an identical procedure was followed, but the primary antibody was omitted (data not shown).

Quantitative real-time reverse transcriptase-polymerase chain reaction (qRT-PCR)

Total RNA extraction from primary cultured hepatocytes, cDNA synthesis and qRT-PCR analysis were performed as previously described [26]. Gene expression mixes for Cx32 (accession number NM_017251.2), GAPDH (accession number NM_017008.3), beta-actin (accession number NM_031144.2) and 18S rRNA (accession number X03205.1) were from Applied Biosystems (USA) with assay ID Rn01641031_s1, Rn99999916_s1, Rn00667869_m1 and Hs99999901_s1, respectively. At indicated time points, Ct-values of Cx32 were normalized to those of GAPDH, beta-actin and 18S rRNA for both the test samples (treated cultures) and the calibrator samples (untreated cultures). The resulting ΔCt-values of the test samples were then normalized to those of the calibrator samples, yielding ΔΔCt. Relative alterations (fold change) in mRNA levels were calculated according to the formula $2^{-(\Delta\Delta Ct)}$.

Statistical analysis

Data were expressed as mean ± standard deviation of at least three independent experiments ($n \geq 3$). Results were evaluated by one-way ANOVA (repeated measures when appropriate), followed by post hoc Bonferroni tests.

Results

Characterization of the cell death response induced by FasL/CHX

To induce cell death, cultures of hepatocytes were exposed for 6 h to FasL (200 ng/ml) and CHX (2 µg/ml), a potent inhibitor of protein synthesis which has been shown to potentiate Fas-mediated cellular responses [27, 28]. Characterization of the cell death response was carried out by combined in situ stainings with Annexin V, Hoechst 33342 and Propidium iodide (Fig. 1a–c). An early event during the commitment of cells to apoptosis is the externalization of phosphatidyl serine in the cell plasma membrane, a process that can be monitored by the phospholipid binding protein Annexin V [29]. In the current experimental setting, however, the number of Annexin V-positive hepatocytes only significantly ($p < 0.05$) increased after 6 h of exposure to FasL/CHX (Fig. 1a). In a subsequent stage of apoptosis, cells display chromatin fragmentation and condensation, which can be detected by the DNA intercalating dye Hoechst 33342 [19, 29]. These hallmarks progressively appeared in our experimental setting, thus demonstrating the deleterious outcome of FasL/CHX (Fig. 1b). Late apoptotic cells typically switch to a rather necrotic appearance, which is associated with disruption of the cell plasma membrane. Propidium iodide only enters cells that have lost cell plasma membrane integrity and thus specifically stains cells undergoing the apoptotic-to-necrotic transition [29]. In line with this, Propidium iodide-positive counts significantly ($p < 0.001$) peaked after 6 h of exposure of hepatocytes to FasL/CHX (Fig. 1c).

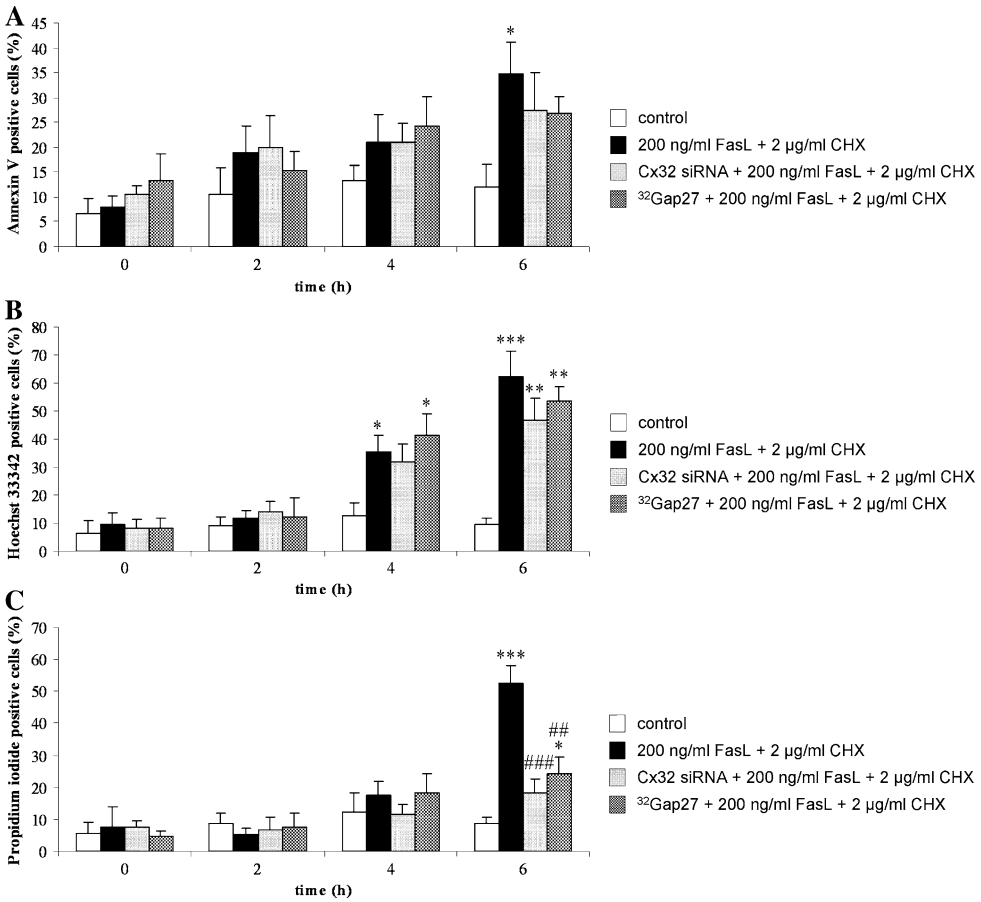

Fig. 1 Characterization of the cell death response induced by FasL/CHX in hepatocytes. Primary hepatocytes were cultivated and cell death was induced as specified in "Materials and methods". In a parallel set of experiments, cells were treated with Cx32 siRNA or ^{32}Gap27 prior to cell death induction. At indicated time points, cells were stained with Annexin V, Hoechst 33342, and Propidium iodide, and subjected to light microscopy and fluorescence microscopy. At least five images per culture dish were taken. The number of cells positive for **a** Annexin V **b** Hoechst 33342 and **c** Propidium iodide was counted in each image and expressed relative to the total number of nuclei present. Data are expressed as mean ± standard deviation of six independent experiments. Results were evaluated by one-way ANOVA followed by post hoc Bonferroni tests. *Asterisks* indicate significant differences compared with the corresponding "control" (untreated) condition per indicated time point ($^{*}p < 0.05$, $^{**}p < 0.01$, $^{***}p < 0.001$). *Number signs* indicate significant differences compared with the corresponding "200 ng/ml FasL + 2 µg/ml CHX" (cell death) condition per indicated time point ($^{\#\#}p < 0.01$, $^{\#\#\#}p < 0.001$)

To further quantify the cell death response, both apoptosis and necrosis were recorded at the activity level. Apoptosis was measured by using Ac-DEVD-AFC, a prototypical, though not exclusive, caspase 3 substrate [19], whereas necrotic activity was assessed by determination of the LDH index, a cytosolic enzyme that leaks into the cell culture medium upon disrupture of the cell plasma membrane [24] (Fig. 2a–b). Caspase 3 activation was previously reported to be a reliable and sensitive marker of apoptosis in primary hepatocytes [18]. Indeed, this parameter already significantly ($p < 0.05$) increased after 2 h and reached a maximum after 4 h (Fig. 2a). By contrast, the LDH index only significantly ($p < 0.001$) increased 6 h after cell death induction (Fig. 2b).

Effects of FasL/CHX on Cx32 expression, localization and function

We used FRAP analysis to analyze the functional state of the gap junctions between the hepatocytes following the induction of Fas-mediated cell death (Fig. 3a–b). Photobleaching was directed in these experiments to Annexin V-positive hepatocytes. We found a continuous decrease in cell–cell dye coupling during the 6 h observation period, becoming statistically significant ($p < 0.01$) after 4 h (Fig. 3b).

Since alterations in GJIC are frequently accompanied by similar changes in connexin expression [6], we next monitored hepatocellular Cx32 protein levels during the time course of FasL/CHX-induced cell death. To this end, immunoblotting and subsequent densitometric analyses were performed (Fig. 4a–b). Unexpectedly, the Cx32 protein amount progressively increased, reaching a maximum level after 6 h of cell death induction (Fig. 4b).

We then investigated whether the increased Cx32 protein levels were associated with alterations in its cellular localization. For this purpose, we prepared Triton X-100 insoluble protein fractions and biotinylated cell surface protein fractions prior to Cx32 immunoblot analyses (Fig. 5a–b). The former is known to contain gap junctional Cx32 whereas the latter indicates Cx32 present in non-junctional plasma membrane regions, i.e., in a hemichannel configuration [30]. As depicted in Fig. 5b, gap junctional Cx32 gradually decreases upon exposure of hepatocytes to FasL/CHX, a finding that could explain the deterioration of GJIC under these conditions (Fig. 3a–b). By contrast, the Cx32 amount in the biotinylated cell surface protein fraction was elevated during cell death, reaching a peak level

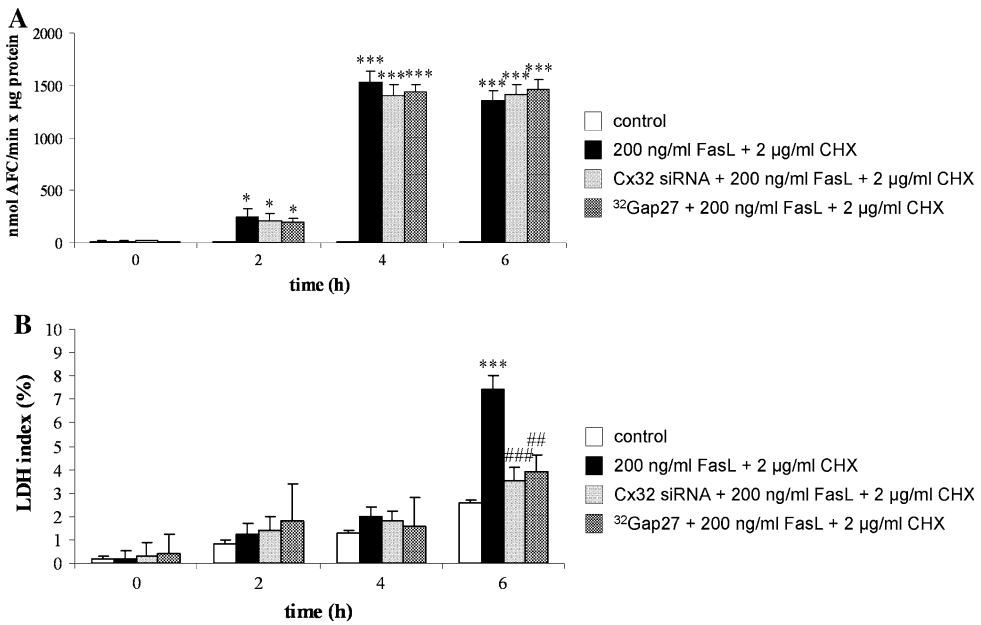

Fig. 2 Modulation of apoptotic and necrotic activities during cell death induced by FasL/CHX in hepatocytes. Primary hepatocytes were cultivated and cell death was induced as specified in "Materials and methods". In a parallel set of experiments, cells were treated with Cx32 siRNA or ^{32}Gap27 prior to cell death induction. At indicated time points, **a** caspase 3-like activity and **b** LDH leakage were measured. Caspase 3-like activity is expressed as nmol AFC/min × µg protein. The LDH index was calculated by the equation (100 × LDH activity in supernatant)/[LDH activity in (supernatant + cells)]. Data are expressed as mean ± standard deviation of six independent experiments. Results were evaluated by one-way ANOVA followed by post hoc Bonferroni tests. *Asterisks* indicate significant differences compared with the corresponding "control" (untreated) condition per indicated time point ($^{*}p < 0.05$, $^{***}p < 0.001$). *Number signs* indicate significant differences compared with the corresponding "200 ng/ml FasL + 2 µg/ml CHX" (cell death) condition per indicated time point ($^{\#\#}p < 0.01$, $^{\#\#\#}p < 0.001$)

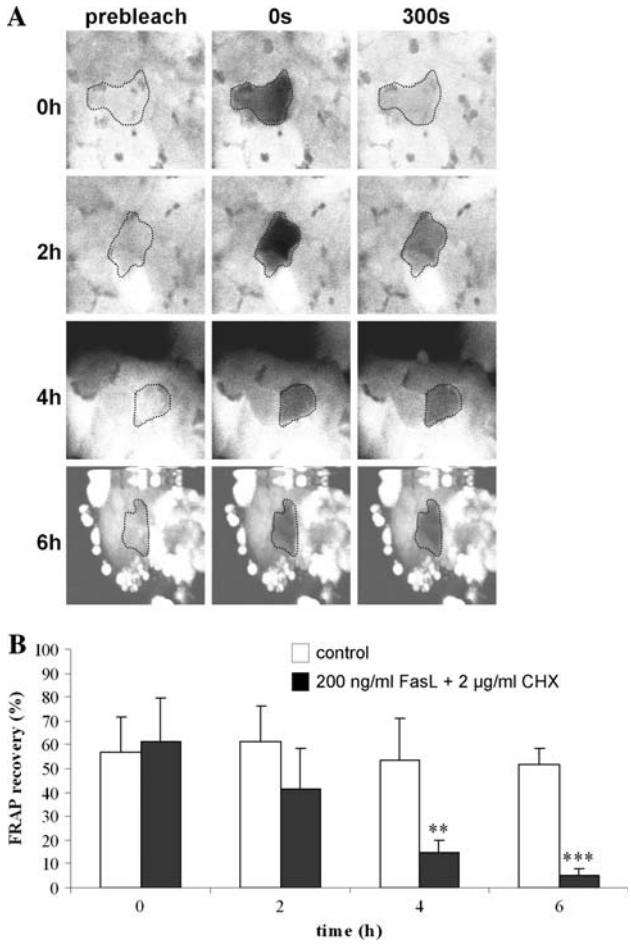

Fig. 3 Effects of FasL/CHX on GJIC between hepatocytes. Primary hepatocytes were cultivated and cell death was induced as specified in "Materials and methods". At indicated time points, cells were subjected to FRAP analysis, whereby a total of 72 pictures were taken, starting 1 min before photobleaching and ending 5 min after photobleaching. **a** Example pictures (magnification ×400) taken at the start of procedure (prebleach), just after photobleaching (0 s) and at the end of the registration period (300 s) are shown. Bleached cells are delineated by *dashed lines*. **b** At least six cells per culture dish were examined. Fluorescence in the bleached cells is expressed as the percentage recovery relative to the prebleach level. Data are expressed as mean ± standard deviation of four independent experiments. Results were evaluated by one-way ANOVA followed by post hoc Bonferroni tests. *Asterisks* indicate significant differences compared with the corresponding "control" (untreated) condition per indicated time point (**$p < 0.01$, ***$p < 0.001$)

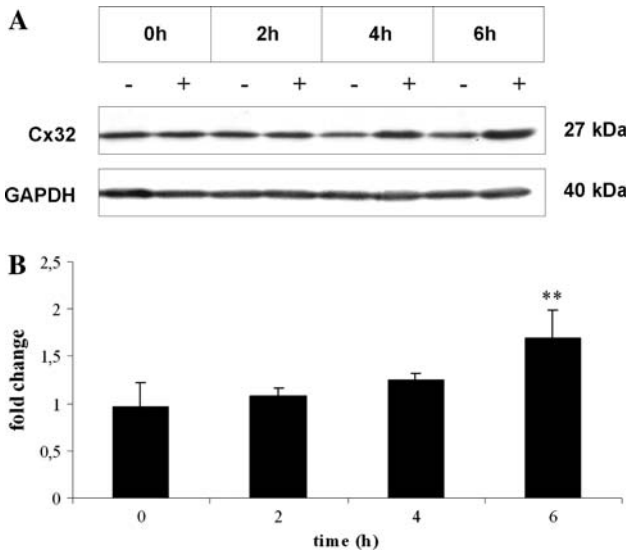

Fig. 4 Effects of FasL/CHX on Cx32 protein levels in hepatocytes. Primary hepatocytes were cultivated and cell death was induced as specified in "Materials and methods". **a** At indicated time points, western blot analysis of Cx32 was performed. **b** For semi-quantification of the results, densitometric analysis was performed. Cx32 signals of cell death-induced cultures (+) were normalized to the corresponding GAPDH signals and are expressed as fold change of the normalized Cx32 signals in control (−) cultures. Data are expressed as mean ± standard deviation of four independent experiments. Results were evaluated by one-way ANOVA followed by post hoc Bonferroni tests. *Asterisks* indicate significant differences compared with the corresponding control (untreated) condition per indicated time point (**$p < 0.01$)

after 6 h (Fig. 5b). Immunocytochemistry analysis further confirmed the increased presence of Cx32 at unapposed cell plasma membrane regions at the end of the cell death process (Fig. 5c). This observation may underlie the overall augmentation in de novo synthesized Cx32 protein in our experimental setting (Fig. 4a–b).

To examine whether the elevated hepatocellular Cx32 production during Fas-mediated cell death is also reflected at the transcriptional level, we performed qRT-PCR analyses, using three housekeeping genes (GAPDH, 18S rRNA, and beta-actin) (Fig. 6a–c). We consistently observed strongly decreased Cx32 gene transcription, whereby Cx32 mRNA levels drastically declined after 2 h of exposure of the hepatocytes to FasL/CHX and remained low until the end of the cell death process (Fig. 6a–c).

Effects of Cx32 siRNA on cell death induced by FasL/CHX

To unravel the relevance of the augmentation in hepatocellular Cx32 protein production, especially towards the late phases of Fas-mediated cell death, we used a mixture of four Cx32 siRNA duplexes (100 nM). Following siRNA treatment, the Cx32 protein amount declined to 30.9 ± 7.5% of the control (untreated) level (Fig. 7a–b). The Cx32 siRNA-treated hepatocytes displayed significantly ($p < 0.05$) decreased FRAP recovery (21.6 ± 6.9% vs 58.2 ± 14.4%) (Fig. 7c), thus confirming that gap junctions composed of Cx32 account for the vast majority of GJIC between hepatocytes. The Cx32 siRNA duplexes also significantly ($p < 0.05$) lowered extracellular ATP release by hepatocytes to 65.1 ± 7.5% of the control level following withdrawal of divalent ions from the cell culture medium (Fig. 7d), which is a well-known protocol to

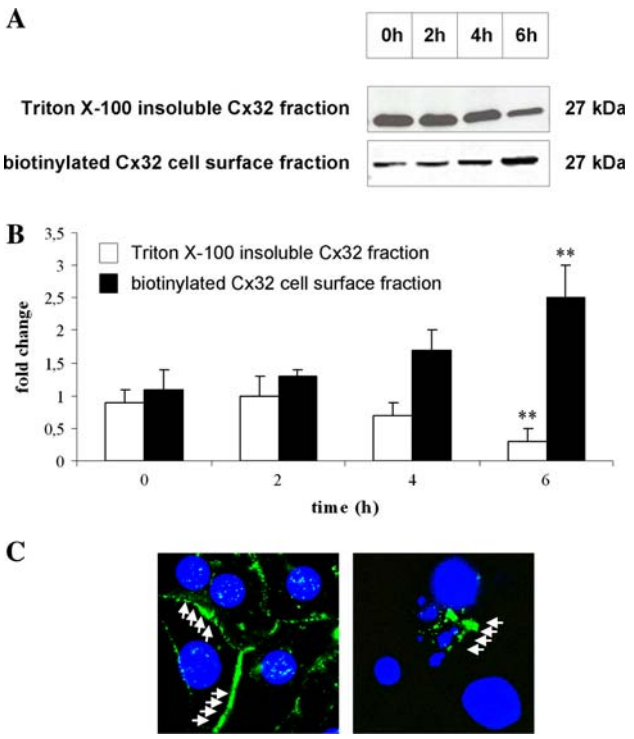

Fig. 5 Effects of FasL/CHX on the localization of Cx32 in hepatocytes. Primary hepatocytes were cultivated and cell death was induced as specified in "Materials and methods". **a** At indicated time points, Triton X-100 insoluble Cx32 fractions and biotinylated Cx32 cell surface fractions were prepared, and were subsequently subjected to Cx32 Western blot analysis. **b** For semi-quantification of the results, densitometric analysis was performed. Data are expressed as mean ± standard deviation of three independent experiments and represent fold change of the Cx32 signals at the start of cell death induction. Results were evaluated by one-way ANOVA followed by post hoc Bonferroni tests. *Asterisks* indicate significant differences compared with the corresponding Cx32 signal at the start of cell death induction (**$p < 0.01$). **c** After 6 h of cell death induction, hepatocyte cultures were subjected to immunocytochemistry analysis, using a primary antibody directed against Cx32 and a fluorescein isothiocyanate-conjugated secondary antibody (*green*; *white arrows*), as specified in "Materials and methods". Nuclear counterstaining was performed with diamidinophenylindole (*blue*). Samples were analyzed by fluorescence microscopy at ×630 magnification. Untreated (control) cultures and treated (cell death) cultures are shown in the *left panel* and *right panel*, respectively, and are representative of three independent experiments

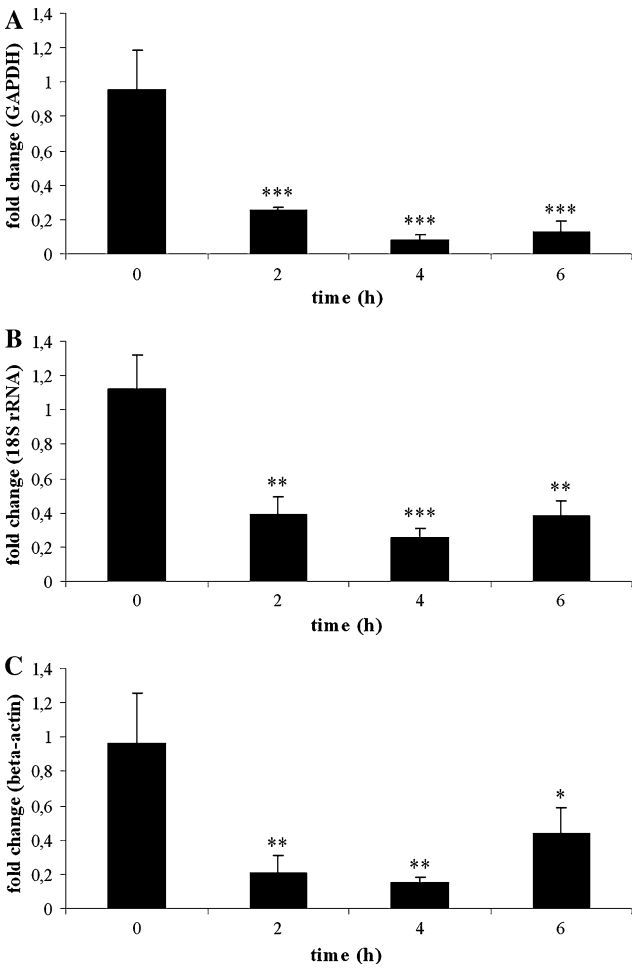

Fig. 6 Effects of FasL/CHX on Cx32 mRNA levels in hepatocytes. Primary hepatocytes were cultivated and cell death was induced as specified in "Materials and methods". At indicated time points, qRT-PCR analysis was performed, using **a** GAPDH, **b** 18S rRNA, and **c** beta-actin as housekeeping genes. Relative alterations (fold change) in Cx32 mRNA levels were calculated according to the $2^{-(\Delta\Delta Ct)}$ method. Data are expressed as mean ± standard deviation of four independent experiments. Results were evaluated by one-way ANOVA followed by post hoc Bonferroni tests. *Asterisks* indicate significant differences compared with the corresponding control (untreated) condition per indicated time point (*$p < 0.05$, **$p < 0.01$, ***$p < 0.001$)

trigger hemichannel opening and thus to measure their functionality [30–32].

When Cx32 gene silencing was performed prior to cell death induction, no changes in the Annexin V-based apoptotic index and its Hoechst 33342-based counterpart were observed (Fig. 1a–b). Caspase 3-like activity also remained unchanged under these conditions (Fig. 2a). However, both the number of Propidium iodide-positive counts (Fig. 1c) and the LDH index (Fig. 2b) were significantly ($p < 0.001$) reduced after 6 h. Experiments using non-targeting siRNA were performed in parallel, whereby no effects on all parameters measured were observed (data not shown). These results indicate that Cx32 plays a role in the late phases of Fas-mediated hepatocellular cell death.

Effects of Cx32 mimetic peptide on cell death induced by FasL/CHX

The increased presence of Cx32 in non-junctional cell plasma membrane regions after 6 h of cell death induction in primary hepatocytes (Fig. 5a–c) as well as the strongly decreased gap junction activity at this time point (Fig. 3a–b), combined with the results obtained by the

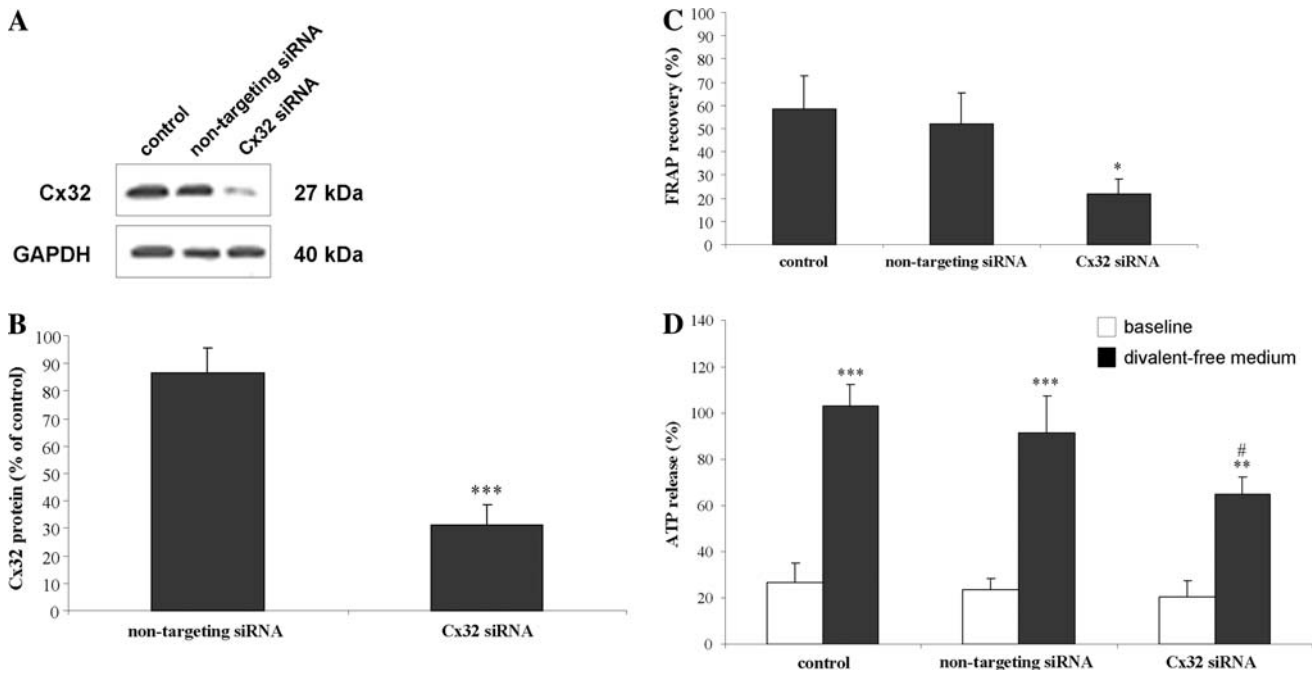

Fig. 7 Efficiency of Cx32 siRNA duplexes in hepatocytes. Primary hepatocytes were cultivated and siRNA-mediated Cx32 gene silencing was performed as outlined in "Materials and methods" section. **a** Cx32 western blot analysis was carried out, followed by densitometric analysis. **b** Cx32 signals of Cx32 siRNA-treated cells and non-targeting siRNA-treated cells were normalized to the corresponding GAPDH signals and are expressed as fold change of the normalized Cx32 signals in control (untreated) cultures. Data are expressed as mean ± standard deviation of four independent experiments. Results were evaluated by one-way ANOVA followed by post hoc Bonferroni tests. *Asterisks* indicate significant differences compared with the control (untreated) condition (***$p < 0.001$). **c** FRAP analysis was performed. At least six cells per culture dish were examined. Fluorescence in the bleached cells is expressed as the percentage recovery relative to the prebleach level. Data are expressed as mean ± standard deviation of four independent experiments. Results were evaluated by one-way ANOVA followed by post hoc Bonferroni tests. *Asterisks* indicate significant differences compared with the control (untreated) condition (*$p < 0.05$). **d** The release of ATP was measured under basal (baseline) and induced (divalent-free medium) conditions, and is expressed as the percentage of ATP release triggered by divalent-free medium in untreated cultures (control). Data are expressed as mean ± standard deviation of three independent experiments. Results were evaluated by one-way ANOVA followed by post hoc Bonferroni tests. *Asterisks* indicate significant differences between the "divalent-free medium" condition and the corresponding "baseline" condition (**$p < 0.01$, ***$p < 0.001$). *Number signs* indicate significant differences between the "divalent-free medium" condition of "Cx32 siRNA" cultures and the "divalent-free medium" condition of "control" cultures ($^{\#}p < 0.05$)

Cx32 siRNA experiments (Figs. 1a–c and 2a–b), suggest that Cx32-based hemichannels, but not their full channel counterparts, are involved in the control of the terminal stages of Fas-mediated hepatocellular cell death. To substantiate this anticipated role for hepatocellular Cx32-originating connexons, we used ^{32}Gap27, a short peptide that mimics a sequence in the second extracellular loop of the Cx32 subunit. Previous research showed that short-term incubations (0.5–6.5 h) with connexin mimetic peptides are sufficient to inhibit hemichannel-related responses, i.e., low extracellular divalent ion-triggered cellular ATP release, in a connexin-specific way, whereas longer exposure regimes (24 h) also result in the reduction of corresponding GJIC [31, 32]. In agreement with this finding, 6.5 h exposure (i.e., 0.5 h pre-incubation followed by 6 h exposure, as required to complete the cell death response) of the hepatocytes to ^{32}Gap27 (0.25 mg/ml) significantly ($p < 0.05$) reduced the ATP release triggered by divalent ion depletion to 62.4 ± 4.8% of the initial level (Fig. 8a). FRAP recovery, reflecting GJIC, remained unchanged under these conditions (Fig. 8b).

At all time points measured, the apoptotic markers Annexin V and Hoechst 33342 were left unaffected when ^{32}Gap27 treatment was initiated 30 min before inducing cell death in primary hepatocytes (Fig. 1a–b). This also held true for the caspase 3-like activity (Fig. 2a). Upon counteracting Cx32 hemichannel-related functioning, however, the peaks in both the Propidium iodide-based necrotic index (Fig. 1c) and the LDH index (Fig. 2b), typically culminating after 6 h of cell death induction, were abolished. These findings are identical to the outcome of the Cx32 siRNA experiments and point to an active role for Cx32 hemichannels in the termination of Fas-mediated hepatocellular cell death.

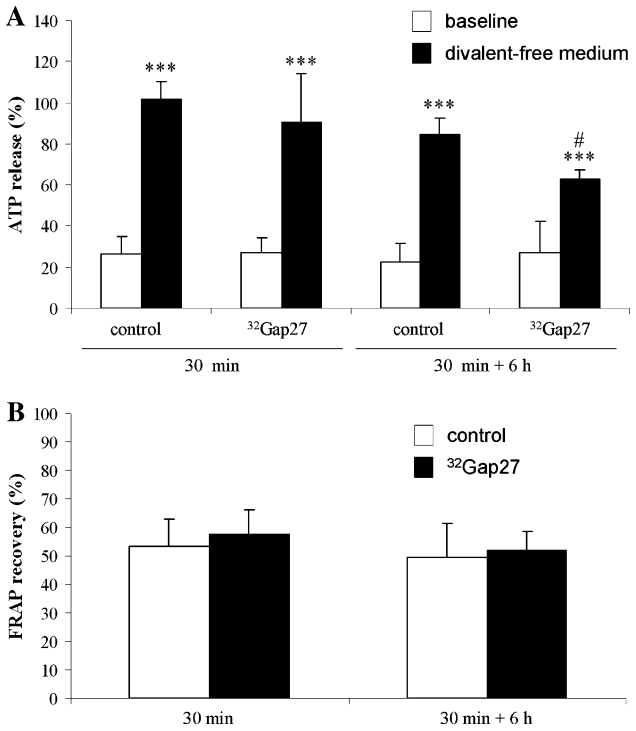

Fig. 8 Efficiency of ^{32}Gap27 in hepatocytes. Primary hepatocytes were cultivated and cells were treated with ^{32}Gap27 (30 min pre-incubation followed by 6 h of exposure) as outlined in "Materials and methods". **a** The release of ATP was measured under basal (baseline) and induced (divalent-free medium) conditions, and is expressed as the percentage of ATP release triggered by divalent-free medium in untreated cultures (control) at 30 min. Data are expressed as mean ± standard deviation of three independent experiments. Results were evaluated by one-way ANOVA followed by post hoc Bonferroni tests. *Asterisks* indicate significant differences between the "divalent-free medium" condition and the corresponding "baseline" condition (***$p < 0.001$). *Number signs* indicate significant differences between the "divalent-free medium" condition of "^{32}Gap27" cultures after 6.5 h and the "divalent-free medium" condition of "control" cultures after 30 min ($^{\#}p < 0.05$). **b** FRAP analysis was performed. At least six cells per culture dish were examined. Fluorescence in the bleached cells is expressed as the percentage recovery relative to the prebleach level. Data are expressed as mean ± standard deviation of three independent experiments. Results were evaluated by one-way ANOVA followed by post hoc Bonferroni tests

Discussion

The aim of this study was to examine the fate of gap junctions in hepatocyte apoptosis. We found that GJIC between cultured hepatocytes drastically decreases upon progression of the FasL/CHX-induced cell death response. This outcome is in line with the recent study of Theiss et al. [33], showing strongly reduced cell–cell coupling between primary lens epithelial cells upon exposure to a number of apoptosis-inducing chemicals, including CHX. Kalvelyte et al. [17] reported that abrogation of GJIC during apoptosis results from the removal of gap junctions and not from their functional closure. Our results can be reconciled with this finding, as we observed a progressive diminution of the gap junctional Cx32 protein pool. Simultaneously, de novo synthesized Cx32 gathered at non-junctional areas of the cell plasma membrane surface, particularly towards the final stages of the cell death process. This modification was not reflected at the transcriptional level. In fact, Cx32 protein and mRNA levels behaved in opposite ways, as the latter rapidly declined during progression of apoptosis. Such disconnection between connexin gene transcription and translation was also observed in apoptosis-primed human osteoblasts and was thought to represent a reflexive adaptation of the connexin mRNA machinery to changes occurring at the downstream protein level [34].

While Cx32 gap junctions seem to play only a minor role in hepatocellular cell death, our data suggest that Cx32 hemichannels could fulfill an important function, especially during the final stage of this process. Such distinctive roles for these Cx32-based channels may suggest differential and even opposite regulation, a feature that has previously been reported for gap junctions and hemichannels composed of Cx43 [35, 36]. The involvement of Cx32 hemichannels in our experimental setting was investigated via four different strategies. Indeed, we applied siRNA technology to silence Cx32 protein synthesis, we performed cell surface biotinylation studies, we used a mimetic peptide to interfere with Cx32 hemichannel functioning and we applied low extracellular divalent ion-triggered cellular ATP release. With respect to that latter, we cannot rule out the participation of alternative ATP release pathways known to be present in hepatocytes, including P_2X_7 receptors [37] and pannexin-containing hemichannels [38], which may explain the incomplete inhibition of ATP release by ^{32}Gap27 in our experiments. Both the inhibition of Cx32 hemichannel-related cellular responses by ^{32}Gap27 and the siRNA-mediated silencing of Cx32 expression had an identical outcome, namely a drop in the LDH index and a reduction of the number of Propidium iodide-positive cells at the end of the cell death process, whereas early apoptotic markers were not affected. Our data are thus consistent with the scenario that Cx32 hemichannels mediate the late phases of FasL/CHX-induced cell death in hepatocytes, by promoting the transition from an apoptotic to a necrotic phenotype. This finding supports the research of Kalvelyte and his group, performed on Cx32-transfected HeLa cells, showing that Cx32 accelerates the transformation of apoptotic cells into a necrotic state, partly depending on the ability to form functional hemichannels [17]. In the same experimental setting, metabolic inhibition, an ischemia-like condition leading to cell death, was recently reported to be associated with the increased formation and activity of Cx32 hemichannels [39]. In a similar way, connexons composed of Cx43 [13, 14, 16, 17] have been reported to propagate apoptotic cell death in a number of cell types.

In conclusion, the current study is the first to demonstrate the presence of functional Cx32 hemichannels in hepatocytes. We showed that these particular cell plasma membrane channels are actively involved in the termination of Fas-mediated cell death in primary hepatocyte cultures. Further research is required to investigate the relevance of these findings in vivo and to examine the involvement of Cx32 hemichannels in other cellular events that constitute the hepatocyte's life cycle known to be governed by Cx32-based gap junctions, including proliferation and differentiation [6].

Acknowledgments The authors wish to thank Mr. Bart Degreef, Mr. Roel Fiey and Miss Sofie Wijthouck for their excellent technical assistance. This work was supported by grants from the Fund for Scientific Research Flanders (FWO-Vlaanderen), the Interuniversity Attraction Poles Program (Belgian Science Policy), the Research Council of the Vrije Universiteit Brussel (OZR-VUB) and the European Union (FP6 projects CARCINOGENOMICS and LIINTOP).

References

1. Maeda S (2000) Mechanisms of active cell death in isolated hepatocytes. In: Berry MN, Edwards AM (eds) The hepatocyte review. Kluwer, Norwell, pp 281–300
2. Malhi H, Gores GJ, Lemasters JJ (2006) Apoptosis and necrosis in the liver: a tale of two deaths? Hepatology 43:S31–S44
3. Malhi H, Gores GJ (2008) Cellular and molecular mechanisms of liver injury. Gastroenterology 134:1641–1654
4. Qiao L, Farrell GC (1999) The effects of cell density, attachment substratum and dexamethasone on spontaneous apoptosis of rat hepatocytes in primary culture. In Vitro Cell Dev Biol Anim 35:417–424
5. Vinken M, Vanhaecke T, Papeleu P, Snykers S, Henkens T, Rogiers V (2006) Connexins and their channels in cell growth and cell death. Cell Signal 18:592–600
6. Vinken M, Henkens T, De Rop E, Fraczek J, Vanhaecke T, Rogiers V (2008) Biology and pathobiology of gap junctional channels in hepatocytes. Hepatology 47:1077–1088
7. Albright CD, Kuo J, Jeong S (2001) cAMP enhances Cx43 gap junction formation and function and reverses choline deficiency apoptosis. Exp Mol Pathol 71:34–39
8. Krysko DV, Leybaert L, Vandenabeele P, D'Herde K (2005) Gap junctions and the propagation of cell survival and cell death signals. Apoptosis 10:459–469
9. Contreras JE, Sanchez HA, Veliz LP, Bukauskas FF, Bennett MV, Saez JC (2004) Role of connexin-based gap junction channels and hemichannels in ischemia-induced cell death in nervous tissue. Brain Res Brain Res Rev 47:290–303
10. Evans WH, De Vuyst E, Leybaert L (2006) The gap junction cellular internet: connexin hemichannels enter the signaling limelight. Biochem J 397:1–14
11. Rodriguez-Sinovas A, Cabestrero A, Lopez D, Torre I, Morente M, Abellan A, Miro E, Ruiz-Meana M, Garcia-Dorado D (2007) The modulatory effects of connexin 43 on cell death/survival beyond cell coupling. Prog Biophys Mol Biol 94:219–232
12. Plotkin LI, Manolagas SC, Bellido T (2002) Transduction of cell survival signals by connexin-43 hemichannels. J Biol Chem 277:8648–8657
13. Decrock E, De Vuyst E, Vinken M, Van Moorhem M, Vranck K, Wang N, Van Laeken L, De Bock M, D'Herde K, Lai CP, Rogiers V, Evans WH, Naus CC, Leybaert L (2009) Connexin 43 hemichannels contribute to the propagation of apoptotic cell death in a rat C6 glioma cell model. Cell Death Differ 16:151–163
14. Ramachandran S, Xie LH, John SA, Subramaniam S, Lal R (2007) A novel role for connexin hemichannel in oxidative stress and smoking-induced cell injury. PLoS ONE 2:e712
15. Takeuchi H, Jin S, Wang J, Zhang G, Kawanokuchi J, Kuno R, Sonobe Y, Mizuno T, Suzumura A (2006) Tumor necrosis factor-alpha induces neurotoxicity via glutamate release from hemichannels of activated microglia in an autocrine manner. J Biol Chem 281:21362–21368
16. Hur KC, Shim JE, Johnson RG (2003) A potential role for Cx43-hemichannels in staurosporin-induced apoptosis. Cell Commun Adhes 10:271–277
17. Kalvelyte A, Imbrasaite A, Bukauskiene A, Verselis VK, Bukauskas FF (2003) Connexins and apoptotic transformation. Biochem Pharmacol 66:1661–1672
18. Gomez-Lechon MJ, O'Connor JE, Lahoz A, Castell JV, Donato MT (2008) Identification of apoptotic drugs: multiparametric evaluation in cultured hepatocytes. Curr Med Chem 15:2071–2085
19. Bai L, Wang J, Yin XM, Dong Z (2003) Analysis of apoptosis: basic principles and procedures. In: Yin XM, Dong Z (eds) Essentials of apoptosis: a guide for basic and clinical research. Humana, Totowa, NJ, pp 239–251
20. Gill GH, Dive D (2000) Apoptosis: basic mechanisms and relevance to toxicology. In: Roberts R (ed) Apoptosis in toxicology. Taylor & Francis, London, pp 1–20
21. Vandenbroucke RE, De Geest BG, Bonne S, Vinken M, Vanhaecke T, Heimberg H, Wagner E, Rogiers V, De Smedt SC, Demeester J, Sanders NN (2008) Prolonged gene silencing in hepatoma cells and primary hepatocytes after small interfering RNA delivery with biodegradable poly(beta-amino esters). J Gene Med 10:783–794
22. Papeleu P, Vanhaecke T, Henkens T, Elaut G, Vinken M, Snykers S, Rogiers V (2006) Isolation of rat hepatocytes. Methods Mol Biol 320:229–237
23. Fraczek J, Deleu S, Lukaszuk A, Doktorova T, Tourwe D, Geerts A, Vanhaecke T, Vanderkerken K, Rogiers V (2009) Screening of amide analogues of Trichostatin A in cultures of primary rat hepatocytes: search for potent and safe HDAC inhibitors. Invest New Drugs 27:338–346
24. Bergmeyer HU (1974) Lactate dehydrogenase. In: Bergmeyer HU (ed) Methods of enzymatic analysis. Academic, New York, pp 574–579
25. Bradford MM (1976) A rapid and sensitive method for the quantitation of microgram quantities of protein utilizing the principle of protein-dye binding. Anal Biochem 72:248–254
26. Vinken M, Henkens T, Vanhaecke T, Papeleu P, Geerts A, Van Rossen E, Chipman JK, Meda P, Rogiers V (2006) Trichostatin A enhances gap junctional intercellular communication in primary cultures of adult rat hepatocytes. Toxicol Sci 91:484–492
27. Rouquet N, Carlier K, Briand P, Wiels J, Joulin V (1996) Multiple pathways of Fas-induced apoptosis in primary culture of hepatocytes. Biochem Biophys Res Commun 229:27–35
28. Ni R, Tomita Y, Matsuda K, Ichihara A, Ishimura K, Ogasawara J, Nagata S (1994) Fas-mediated apoptosis in primary cultured mouse hepatocytes. Exp Cell Res 215:332–337
29. Foster JR (2000) Detection and biomarkers of apoptosis. In: Roberts R (ed) Apoptosis in toxicology. Taylor & Francis, London, pp 213–232
30. Schalper KA, Palacios-Prado N, Orellana JA, Saez JC (2008) Currently used methods for identification and characterization of hemichannels. Cell Commun Adhes 15:207–218

31. Leybaert L, Braet K, Vandamme W, Cabooter L, Martin PE, Evans WH (2003) Connexin channels, connexin mimetic peptides and ATP release. Cell Commun Adhes 10:251–257
32. De Vuyst E, Decrock E, Cabooter L, Dubyak GR, Naus CC, Evans WH, Leybaert L (2006) Intracellular calcium changes trigger connexin 32 hemichannel opening. EMBO J 25:34–44
33. Theiss C, Mazur A, Meller K, Mannherz HG (2007) Changes in gap junction organization and decreased coupling during induced apoptosis in lens epithelial and NIH-3T3 cells. Exp Cell Res 313:38–52
34. Sharrow AC, Li Y, Micsenyi A, Grisworld RD, Wells A, Monga SS, Blair HC (2008) Modulation of osteoblast gap junction connectivity by serum, TNFalpha, and TRAIL. Exp Cell Res 314:297–308
35. De Vuyst E, Decrock E, De Bock M, Yamasaki H, Naus CC, Evans WH, Leybaert L (2007) Connexin hemichannels and gap junction channels are differentially influenced by lipopolysaccharide and basic fibroblast growth factor. Mol Biol Cell 18:34–46
36. Retamal MA, Froger N, Palacios-Prado N, Ezan P, Saez PJ, Saez JC, Giaume C (2007) Cx43 hemichannels and gap junction channels in astrocytes are regulated oppositely by proinflammatory cytokines released from activated microglia. J Neurosci 27:13781–13792
37. Gonzales E, Prigent S, Abou-Lovergne A, Boucherie S, Tjordmann T, Jacquemin E, Combettes L (2007) Rat hepatocytes express functional P2X receptors. FEBS Lett 581:3260–3266
38. Bruzzone R, Hormuzdi SG, Barbe MT, Herb A, Monyer H (2003) Pannexins, a family of gap junction proteins expressed in brain. Proc Natl Acad Sci USA 100:13644–13649
39. Sanchez HA, Orellana JA, Verselis VK, Saez JC (2009) Metabolic inhibition increases activity of connexin-32 hemichannels permeable to Ca^{2+} in transfected HeLa cells. Am J Physiol Cell Physiol 197:C665–C678